Utilisation of Processing and Stability Maps in the Definition of the Hot Forging Conditions of MMCs.

P. Cavaliere[1], A. Forcellese[1], S.M. Roberts°

[1]*Department of Mechanics, University of Ancona, Via Brecce Bianche, 60131 Ancona, Italy*
°*Department of Materials Science and Metallurgy, University of Cambridge, UK*

SUMMARY: A procedure to establish the optimum hot forging conditions needed to produce a car component in Al-MMCs is proposed. Hot formability studies on Al-6061/Al_2O_3/10p composite were used to develop processing and stability maps. In the 'safe' region of the processing map, the most favourable forming window was defined as being over temperature and strain rate ranges of 450-500°C and 0.03-0.3 s^{-1}, respectively. These conditions were used to define the optimum forging parameters by FEM analysis. For the suspension arm geometry, a die speed of 18 mm/s, and initial die and billet temperatures of 450 and 500°C were found to best fit the nominal constraints of temperature and strain rate distributions in the workpiece imposed by the optimal processing window. The validity of the proposed approach was confirmed by the experimental damage measurements.

KEYWORDS: Al-MMCs, Damage model, FEM, Forging, Processing map, Stability map.

1. INTRODUCTION

In the automotive industry, due to pressures deriving from government regulations, the main target is the reduction in fuel car consumption and the associated reduction in harmful engine emissions. The replacement of traditional materials by lighter metals such as aluminium alloys is desirable. However, aluminium alloys are not sufficiently stiff or strong to be used in many situations and so reinforcement is necessary. Discontinuously reinforced aluminium alloy matrix composites (Al-MMCs) are among the most promising candidate materials for this purpose. Unfortunately, such materials are difficult to form due to their intrinsic poor ductility deriving from the presence of the undeformable reinforcing phase, usually SiC or Al_2O_3 particles. Consequently, the production of sound components is strongly dependent on the forming parameters. Forming conditions can be more easily optimised if models, that describe the evolution of damage, are developed.

The present paper aims to establish the optimum forging parameters needed to produce an automotive component from Al-MMC. To this purpose, a combined approach based on both the processing map and the critical strain rate damage model is proposed.

2. THE DYNAMIC MATERIAL MODEL

Processing and stability maps are a helpful guide in the determination of processe conditions leading to defect-free components. They are based on a dynamic material model (DMM) which considers metal-forming systems as energy manipulators[1-3]; the power, generated by a source, is transmitted through the dies to the deforming material. This power is dissipated both by plastic work and dynamic processes occurring during deformation such as recovery, recrystallization, phase transformation, etc., and by damage mechanisms such as cavitation and cracking. In the DMM material behaviour is modelled in terms of power dissipated by metallurgical mechanisms defined as:

$$J=\sigma\dot{\varepsilon}\, m/(m+1) \qquad (1)$$

where σ is the equivalent stress, $\dot{\varepsilon}$ is the equivalent strain rate and m ($= \partial \log\sigma / \partial \log\dot{\varepsilon}\big|_{\varepsilon,T}$) is the strain rate sensitivity coefficient. The maximum value of J is obtained when the deforming material acts as a linear dissipator (i.e. m=1 $\Rightarrow J_{max}=\sigma\dot{\varepsilon}/2$). Under this condition, one-half of the power applied to the workpiece is dissipated by the operative deformation mechanisms. Usually m<1 and J< J_{max}. The capacity for power dissipation can be measured by the efficiency of dissipation (η) defined as:

$$\eta = \frac{J}{J_{max}} = \frac{2\,m}{m+1} \qquad (2)$$

The higher η, the more effective are the processes occurring during deformation in dissipating power.

The temperature sensitivity of flow stress is taken into account by the entropy rate ratio (s) given by the relationship:

$$s = \frac{\dot{S}_{sys}}{\dot{S}_{app}} = \frac{1}{T}\frac{\partial \ln\sigma}{\partial (1/T)}\bigg|_{\varepsilon,\dot{\varepsilon}} \qquad (3)$$

where $\dot{S}_{sys}$ is the rate of entropy produced by the system, $\dot{S}_{app}$ is the rate of entropy applied to the system during deformation, ε is the equivalent strain and T is the absolute temperature.

Since damage mechanisms also contribute to the value of η, it is necessary to identify the 'safe' regions where no damage occurs, i.e. where the plastic flow is stable. The stability criteria derive from the theoretical requirement that the energy of the system decreases continuously. Besides the condition that m should be greater than 0, which is usually achieved under hot forming conditions, and s should be greater than 1, derived from the observation that all the irreversible processes are associated with a net increase in entropy, the following relationships are used to identify the stable plastic flow regions:

$$\left.\frac{\partial \eta}{\partial \log \dot{\varepsilon}}\right|_{\varepsilon,T} < 0 \quad (4)$$

$$\left.\frac{\partial s}{\partial \log \dot{\varepsilon}}\right|_{\varepsilon,T} < 0 \quad (5)$$

A high value of the strain rate sensitivity coefficient reduces the tendency for plastic flow localisation and hinders necking and shear band formation. Equation 4 requires that, for stable plastic flow, the power dissipation efficiency must decrease with increasing strain rate, that is the strain rate sensitivity coefficient must decrease with increasing strain rate. In fact, if strain rate increases in a given region of the workpiece, the flow stress also increases owing to the positive m value. If m increases with increasing strain rate, flow stress undergoes a further increase. Such a strong increase in flow stress leads to a non-uniform stress field with marked plastic flow localisation. On the contrary, a decrease in m with increasing strain rate leads to a plastic flow condition that leads to a more uniform stress state in the deforming material. The stability criterion given by Equation 5 requires that the rate at which entropy increases decreases with increasing strain rate. In reality, when the strain rate increases, flow softening due to adiabatic heating causes a decrease in flow stress. If the entropy rate ratio increases with increasing strain rate, a further decrease in flow stress will occur. Such a marked flow softening can lead to severe plastic flow localisation and adiabatic shear bands.

Equation 2 defines the strain rate and temperature ranges with the highest capacity for power dissipation; Equations 4 and 5 provide the necessary, but not sufficient, strain rate and temperature conditions for stable plastic flow. Such equations are probabilistic indicators of the intrinsic hot formability of a material. If they are not realised, the corresponding plastic flow instabilities can be reduced by a proper definition of the die geometry, i.e. by designing the die cavity so that a stress state characterised by a highly compressive hydrostatic stress component, or by reduced tensile stresses, is created in the workpiece.

3. THE PROPOSED APPROACH

In the present approach to metal-forming process design, the forming parameters are selected using as a guide the ‘safe’ region of the processing map characterised by the highest level of the power dissipation efficiency. The temperature and strain rate distributions within the workpiece, for a given die geometry, predicted by Finite Element Method (FEM) simulations using different forming parameters, are compared with the nominal ranges defined by the selected processing window. The parameters that best fit the constraints imposed by the processing window represent, in terms of intrinsic formability of the material, the conditions that minimise the probability of the occurrence of damage mechanisms.

4. MATERIAL AND EXPERIMENTAL TECHNIQUES

4.1 Material

The particle-reinforced aluminium alloy matrix composite used in the present work is Al-6061/Al_2O_3/10p supplied by Duralcan Co., USA (Duralcan designation: W6A.10A). It was produced by mixing 10 vol% of Al_2O_3 particles, having an average size of 7 µm, into molten AA 6061 aluminium alloy. After casting, billets were pre-homogenised at 570°C for 4 h and cooled at 200°C/h. They were then hot extruded into 55 and 80 mm diameter rods.

4.2 Compression tests

The hot deformation behaviour of Al-6061/Al_2O_3/10p composite was studied by axisymmetric compression tests performed, using a servohydraulic computer-controlled testing machine, in the temperature and strain rate ranges of 350-500°C and 0.001-1.16 s^{-1}, respectively. Cylindrical samples with an initial diameter of 12 mm and an initial height of 18 mm were obtained by EDM. The samples and the loading platens were heated before testing in a resistance furnace with a total heating time of 90 min, consistent with the industrial forging practice. An aquous suspension of graphite (Renite S-28™) was used to reduce the frictional effects at the workpiece-die interfaces. The equivalent stress-equivalent strain data were deduced from the load versus stroke data according to the relationships reported in reference [4]. The equivalent stress was corrected for the increase in friction and in temperature due to deformation induced heating (for $\dot{\varepsilon} \geq 0.1$ s^{-1}).

4.3 Forging trials

The upper transversal arm (Fig. 1) of a multilink suspension for an automotive application was forged. The forging sequence consists of two steps: a preforming process in which the billet is bent followed by a closed-die forging that leads to the final shape.

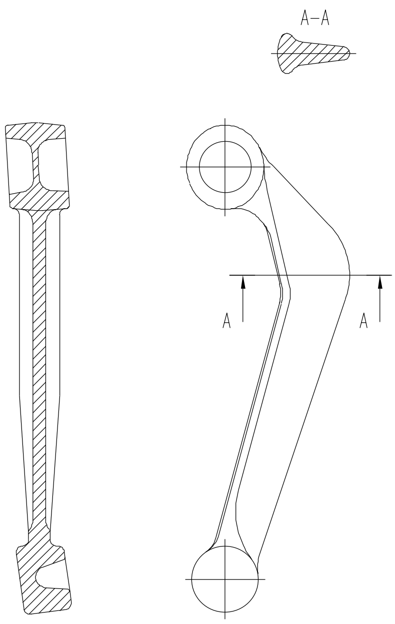

Fig. 1: The forged suspension arm component (length: 340 mm).

Each extruded billet in Al-6061/Al_2O_3/10p, with a diameter of 55 mm and a length of 390 mm, was heated at 475°C for 2 h before preforming. After the first step each workpiece was heated at 500±10°C for 2 h prior to closed-die forging. The temperature was checked using a pyrometer just before operation. The average upper and lower die temperatures were about 325°C and 320°C, respectively; these values were continuously monitored throughout the trials by embedded thermocouples. The optimum lubrication conditions were found to be a combination of Renite S-28™ sprayed between each operation, and animal grease mixed with lead oxide 'painted' on the dies every third or fourth forging. The forgings were obtained on a hydraulic press with a piston diameter of 1450 mm and a capacity of 5000 t at 300 bar. The average pressure was 180 bar and the pressing time was about 8 s; the die speed was about 18 mm/s.

4.4 Microstructural characterisation

The extent and location of damage in the crank section of the upper transversal arm was mapped using an image analysis technique based on optical microscope images. The very small size of voids and their location at the reinforcing particle-matrix interfaces, where Mg_2Si precipitates are also present, made the damage measurements very difficult. Damage was quantified by the ratio between the number of particles associated with voids and the total number of particles investigated (Pv%). A second damage parameter was given by the ratio between the number of voids per unit of area in the forging (N) and the number of voids per unit of area in the undeformed material (Na) [5]. As such, the ratio N/Na indicates the amount of damage accumulated during the process in terms of the damage prior to forging. The change in damage level is thus monitored, indicating the influence of the processing state on the observed damage.

5. RESULTS AND DISCUSSION

5.1 Processing and stability maps

Equivalent stress-equivalent strain data for Al-6061/Al_2O_3/10p demonstrates a weak influence of strain and a strong influence of strain rate and temperature on flow stress [4], as typically observed in aluminium alloys. The data were used to calculate the strain rate sensitivity coefficient. At each strain and temperature, the $\log\sigma$-$\log\dot{\varepsilon}$ data were fitted using a third order regression; a dependency of the strain rate sensitivity coefficient on strain rate was also assumed. The map of the power dissipation efficiency, expressed in terms of strain rate and temperature, shows three different processing windows (Fig. 2):

- window I, in the temperature and strain rate ranges of about 350-400°C and 0.1-1.16 s^{-1}, characterised by the lowest power dissipation efficiency;

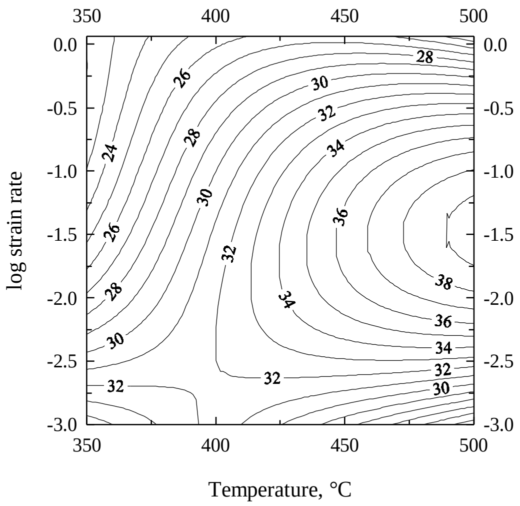

Fig. 2: Map showing the power dissipation efficiency contours for Al-6061/Al_2O_3/10p composite[6].

- window II, in the temperature and strain rate ranges of about 450-500°C and 0.03-0.3 s^{-1}, characterised by the highest power dissipation efficiency;
- window III, in the temperature and strain rate ranges of about 350-400°C and 0.001-0.003 s^{-1}, characterised by intermediate power dissipation efficiency values.

The occurrence of the plastic flow stability was assessed by Equations 4 and 5. Equation 4 is not satisfied in the temperature and strain rate ranges of about 430-500°C and 0.001-0.025 s^{-1} (Fig. 3); this indicates a plastic flow instability. Such an unstable region can be attributed to the diffusional void growth at the matrix-particle interfaces that is the mechanism governing damage at low strain rates and high temperatures [6]. This causes a reduction in flow stress that decreases, for a given temperature, with increasing strain rate and, for a given strain rate, with decreasing temperature. This flow stress behaviour produces an increase in the strain rate sensitivity coefficient with increasing strain rate and, therefore, a non-uniform stress state leading to an instability in the plastic flow. This was confirmed by the occurrence of several very small voids at the reinforcing particle-matrix interfaces in the compression-tested samples deformed within the unstable plastic flow region [4].

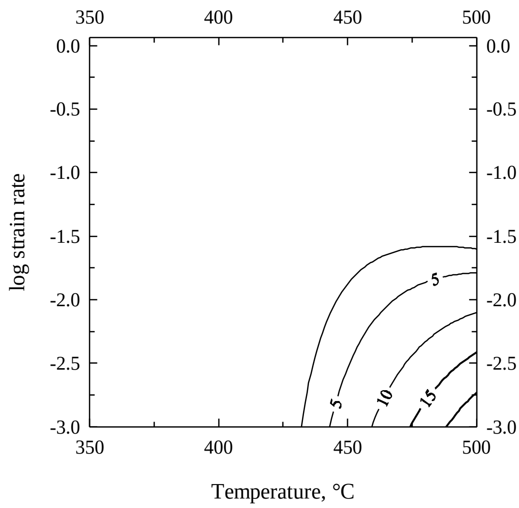

Fig. 3: Map showing the unstable plastic flow region $(\partial\eta/\partial\log\dot{\varepsilon} > 0)$ *for Al-6061/Al_2O_3/10p composite[6].*

5.2 The definition of the forging parameters

The 'safe' region II (T=450-500°C, $\dot{\varepsilon}$ =0.03-0.3 s^{-1}) in the processing map was used to select the nominal forming parameters of both preforming and forging operations for producing the upper transversal arm (Fig. 1) in Al-6061/Al_2O_3/10p composite. Since the stress and strain states induced by the closed-die forging are more severe than those induced by the initial bending, the optimisation focused on the forging stage. Only the cross section across the crank of the suspension arm component was simulated (i.e. across A-A in Fig. 1). The combination of the distortion due to the forming of the elbow followed by the subsequent closed-die operation in this section of the component suggests that the internal damage is expected to be the highest. For the suspension arm die geometry, a die speed of 18 mm/s, and initial die and billet temperatures of 450 and 500°C, respectively, are the forging parameters that best fit the nominal constraints of temperature and strain rate distributions within the workpiece imposed by the processing window II. As already mentioned, the forging parameters must be selected in order to avoid the damage mechanisms occurring at the low strain rates and high temperatures that are not taken into account by the critical strain rate model; such conditions were obtained by preventing the strain rate from falling below 0.03 s^{-1}

and the temperature rising above 500°C. The damage predicted under such forging conditions by the critical strain rate model is shown in fig. 4.a [7]. It can be observed that a very small damaged area is expected in the region of the forging near the flash. This is due to the high $\dot{\varepsilon}$ values in this region which exceed the upper limit of the reference range (0.3 s^{-1}) given by the window II of the processing map.

5.3 Validation of the predictive model

In order to validate the predictive damage capability of the procedure based on the processing and stability maps, the component was forged under conditions for which internal damage was expected to occur. Closed-die trials were carried out with a die temperature of about 320°C whilst the billet temperature (500°C) and the die speed (18 mm/s) were taken to be equal to the optimal values obtained in the previous section. The FEM simulation performed under these conditions has shown that the workpiece temperature varies from about 320 to 480°C. These conditions correspond to the processing window IV (T=320-480°C, $\dot{\varepsilon}$ =0.03-0.3 s^{-1}). In this window, despite the plastic flow still being stable (Fig. 3), the probability of occurrence of internal damage is higher than in the window II. This is as a result of the level of the stability parameters of the Equations 4 and 5 being closer to the

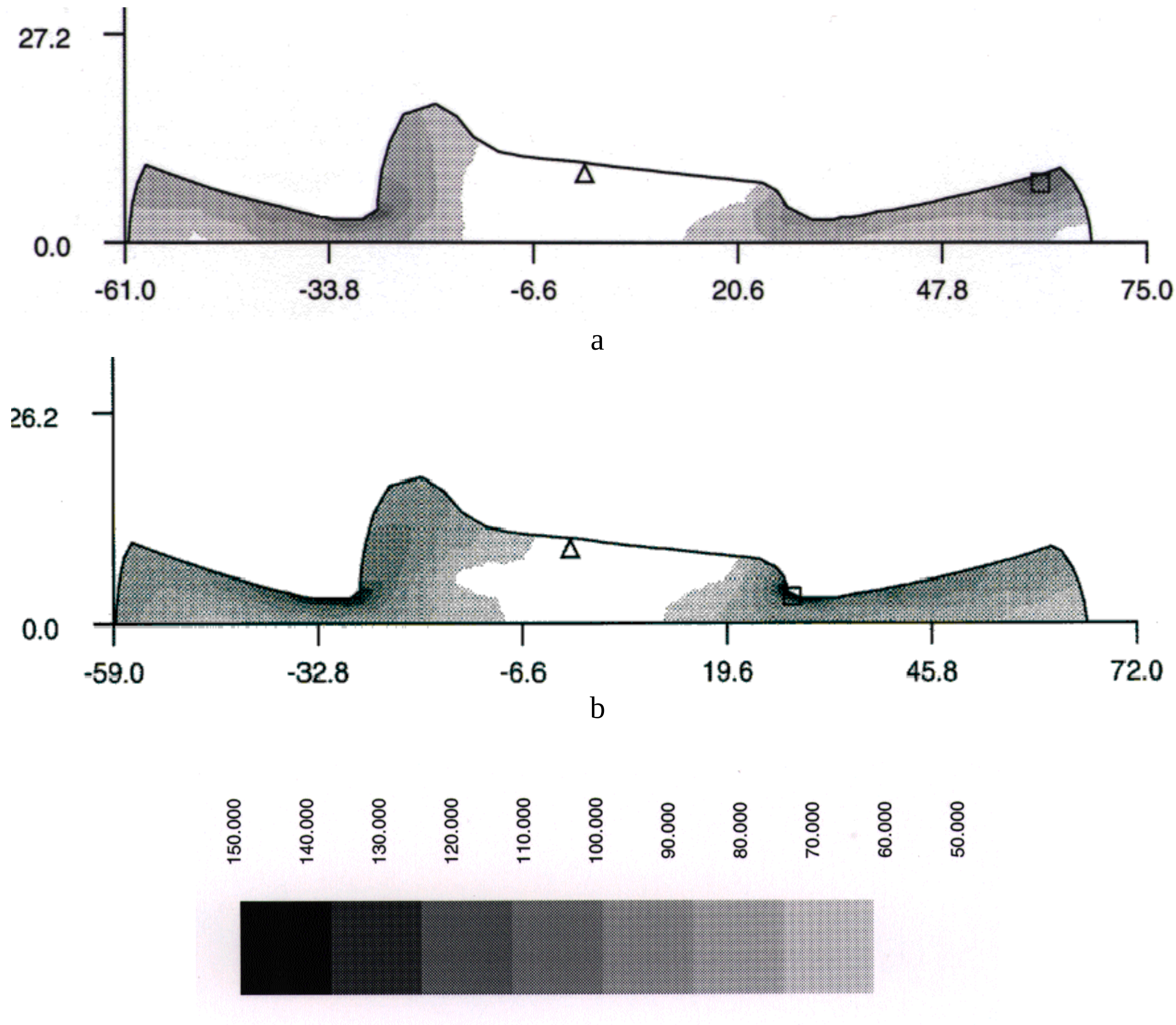

Fig. 4: Maps showing the propensity for damage as characterised by the strain rate/critical strain rate ratio for:

a) *a die speed of 18 mm/s, initial die and billet temperatures of 450 and 500°C;*

b) *a die speed of 18 mm/s, initial die and billet temperatures of 320 and 500°C [7].*

instability condition than in window II. Moreover, the processing window IV is characterised by power dissipation efficiency values that are lower than those of the optimum window II; therefore, it can be assumed that the dynamic restoration mechanisms taking place under the temperature and strain rate conditions given by window IV are less effective in recovering ductility than those occurring under the conditions of window II. In the temperature and strain rate conditions given by the processing window IV the critical strain rate model successfully predicts internal damage in the flash area (Fig. 4.b) [7]. This behaviour is confirmed by the experimental damage measurements (Pv% and N/Na parameters) performed in different positions of the crank cross section of the upper transversal arm (Fig. 5), forged at an initial billet temperature of about 500°C, initial lower and upper die temperatures of about 325 and 320°C, respectively, with a die speed of 18 mm/s (Table I). Fig. 6 shows the comparison between measured and predicted damage: both the parameters used to 'measure' damage show the same behaviour. A strong correlation is observed between the measured and predicted damage values. The high level of damage in the regions B and G can be attributed to the high values of strain rate in the corners close to the flash. Such values were successfully predicted by the critical strain rate model. In regions C and D the primary cause of damage would appear to be the tensile stress. Whilst areas C and D were indicated by the critical strain rate model to be the next most

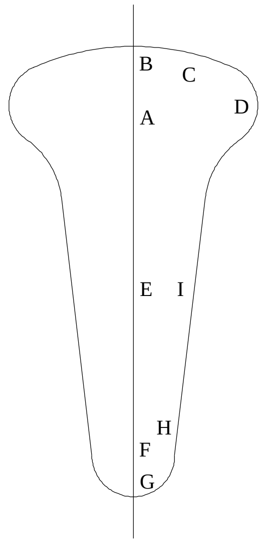

Fig. 5: Positions of the crank cross section of the suspension arm component where damage was measured.

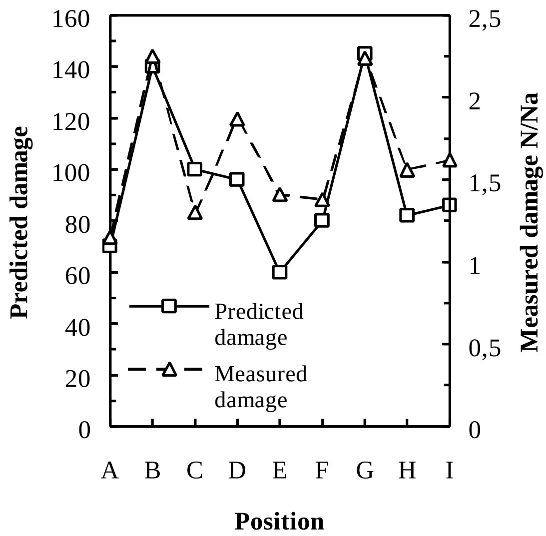

Fig. 6: Comparison between the predicted propensity for damage (arbitrary units) and the measured damage.

Table I: Damage measured in different positions of the crank cross section of the suspension arm component.

Position	A	B	C	D	E	F	G	H	I
Pv%	18	35	16	27	17	17	30	23	22
N/Na	1.15	2.25	1.30	1.87	1.41	1.38	2.24	1.56	1.62

susceptible to damage, the levels predicted are less satisfactory.

Figure 7 shows the SEM microstruture images taken in the C and D zones of the crank section of the forged component in accord with the theory explaned before. The zones with high levels of damage shows two different mechanisms: an high level of void formation at the particle matrix interfaces at the higher temperatures investigated and the particle fracture in the lower temperature rage.

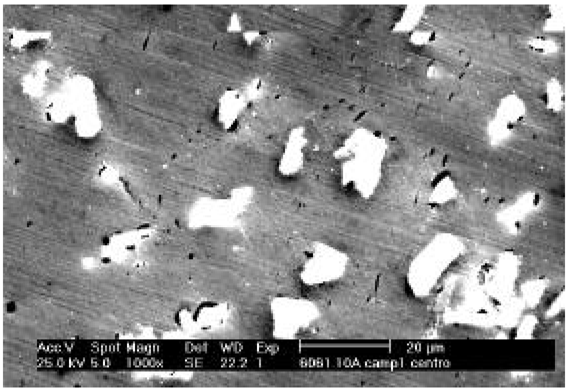

a)

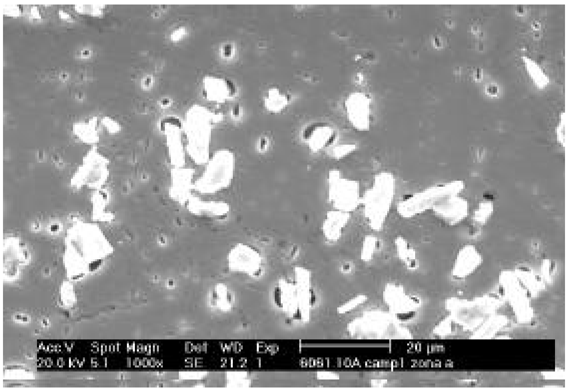

b)

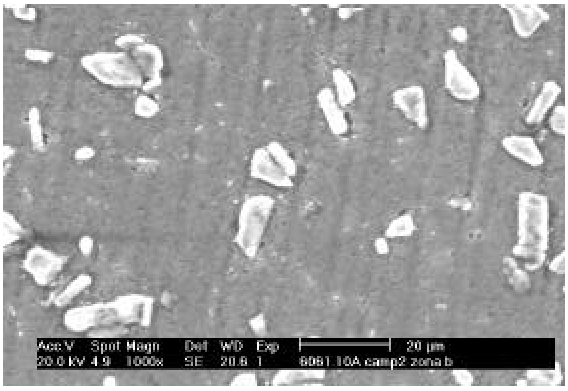

c)

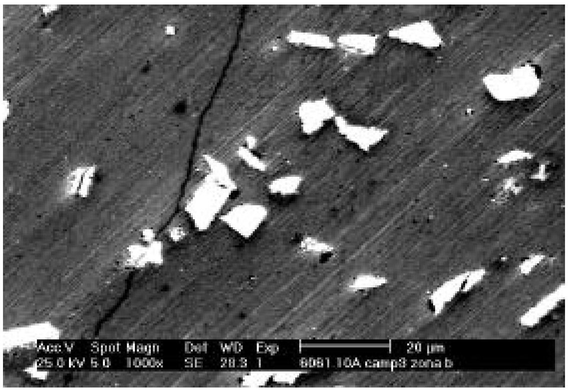

d)

Fig. 7: SEM micrographs showing damage in the crank section of the suspension arm in terms of void formation at the matrix-particle interfaces at:

a) zone E showing an high void formation;
b) zone A showing an high damage level;
c) zone B with a limited damage level in terms of void formation;
d) zone B showing damage in terms of particle cracking.

6.CONCLUSIONS

A combined procedure based on the processing and stability maps and the critical strain rate model for selecting the optimum parameters to forge a suspension arm component in Al-6061/Al_2O_3/10p composite was proposed. The processing and stability maps were shown to be a very effective guide for optimisation the choice of the forging parameters, in terms of billet and die temperatures and die speed. The utilisation of the critical strain rate damage model allows a more precise and safer choice of the forging conditions and a faster route to forge process design.

ACKNOWLEDGEMENTS

The present work has been carried out with funding from the BRITE-EURAM project "Forging of Aluminium Metal Matrix Composites for Automotive Applications" (Contract n. BRE2-CT92-0177). The authors would like to thank their partners on this project: Risø National Laboratory, Roskilde, Dk (H. Lilholt, T.M. Nilsson, Y.L. Lin), Alcan International Ltd, Banbury, UK (P. Enright, A. Owen, R. Grimes, R. Dickson), Stampal SpA, Caselette, I (G.L. Chiarmetta), U.E.S. Garringtons, Bromsgrove, UK (P. Williams), Centro Ricerche Fiat, Orbassano, I (C. Mus, A. Fuganti, L. Lorenzi), and UMIST, Manchester, UK (F.J. Humphreys, P.B. Prangnell, S.J. Barnes).

REFERENCES

1. Gegel, H.L., "Material Behaviour Modeling - An Overview", *Proceedings Symposium on "Experimental Verification of Process Models"*, Metals Congress, C.C. Chen Ed., ASM, Metals Park, OH, September 21-23, 1983, pp. 3-32.

2. Gegel H.L., Malas, J.C., Doraivelu, S.M. and Shende, V.A., "Modeling Techniques Used in Forging Process Design", *Metals Handbook*, 9th Edition, ASM, Metals Park, OH, Vol. 14, 1987, pp. 417-438.

3. Prasad Y:V:R:K:, Sasidhara S., "Hot working guide" (A compendium of processing maps), ASM, Metals Park, OH, 1997.

4. Withers, P.J., Lorentzen, T. and Stobbs W.M., "A Study of the Relation Between the Internal Stresses and the External Loading Response in Al/SiC Composites", *Proceedings 7th International Conference on Composite Materials (ICCM-7)*, Beijing, China, 1989, Vol. 1, pp. 429-434.

5. Roberts, S.M., Kusiak, J., Withers, P.J., Barnes, S.J. and Prangnell, P.B., "Numerical Prediction of the Development of Particle Stress in Forging of Aluminium Metal Matrix Composites", *Journal of Materials Processing Technology*, Vol. 60, 1996, pp 711-718.

6. De Sanctis, A.M., Evangelista, E. and Forcellese, A., "Assessment of the Forging Conditions of 6061/Al_20_3/10p Using Processing Maps and Stability Criteria, *Key Engineering Materials*, Vol. 127-131, Part 1, Trans Tech Publications, 1997, pp. 525-532.

7. Forcellese A., Gabrielli F., Roberts S.M., Withers P.J., "Hot forging of a Suspension Arm Component in Al-MMC for Automotive Applications". Proceedings of the 11th International Conference on Composite Materials (ICCM-11), M.L. Scott Ed., Gold Cost, Queensland, Australia, July 14-18, 1997, Vol.III, pp. 143-153.